Quantitative Measurements of Autofluorescence with the Scanning Laser Ophthalmoscope

François Delori,[1,2] *Jonathan P. Greenberg,*[3] *Russell L. Woods,*[1,2] *Jörg Fischer,*[4] *Tobias Duncker,*[3] *Janet Sparrow,*[3] *and R. Theodore Smith*[3,5]

Purpose. To evaluate the feasibility and reliability of a standardized approach for quantitative measurements of fundus autofluorescence (AF) in images obtained with a confocal scanning laser ophthalmoscope (cSLO).

Methods. AF images (30°) were acquired in 34 normal subjects (age range, 20–55 years) with two different cSLOs (488-nm excitation) equipped with an internal fluorescent reference to account for variable laser power and detector sensitivity. The gray levels (GLs) of each image were calibrated to the reference, the zero GL, and the magnification, to give quantified autofluorescence (qAF). Images from subjects and fixed patterns were used to test detector linearity with respect to fluorescence intensity, the stability of qAF with change in detector gain, field uniformity, effect of refractive error, and repeatability.

Results. qAF was independent of detector gain and laser power over clinically relevant ranges, provided that detector gain was adjusted to maintain exposures within the linear detection range (GL $<$ 175). Field uniformity was better than 5% in a central 20°-diameter circle but decreased more peripherally. The theoretical inverse square magnification correction was experimentally verified. Photoreceptor bleaching for at least 20 seconds was performed. Repeatability (95% confidence interval) for same day and different-day retests of qAF was $\pm$6% to $\pm$14%. Agreement (95% confidence interval) between the two instruments was $<$11%.

Conclusions. Quantitative AF imaging appears feasible. It may enhance understanding of retinal degeneration, serve as a diagnostic aid and as a sensitive marker of disease progression, and provide a tool to monitor the effects of therapeutic interventions. (*Invest Ophthalmol Vis Sci.* 2011;52:9379–9390) DOI:10.1167/iovs.11-8319

The autofluorescence (AF) of the fundus principally emanates from RPE lipofuscin.[1] Lipofuscin is a byproduct of the visual cycle and is a complex mixture of bisretinoids (including A2E) and their oxidized forms.[2] Defects in photoreceptor genes can have a direct impact on RPE lipofuscin levels, such as is the case for ABCA4-related retinal disorders.[3–5] Several adverse effects of RPE lipofuscin has been demonstrated in vitro, including generation of free radicals,[6,7] lysing of cell membrane,[8,9] photoinduced apoptosis,[10,11] and photooxidation-associated complement activation.[12] These deleterious effects may play a role in the pathogenesis of age-related macular degeneration (AMD) and some retinal dystrophies.[13]

Fundus AF has been quantified noninvasively by fluorometry[14] in normal subjects,[1,15] patients with AMD,[16] and those with recessive Stargardt's disease.[17] However, fluorometry did not enjoy broad clinical use, in part because of its restricted availability, but also because of the difficulty in obtaining measurements from discrete areas of pathology in the presence of eye movements.

Fundus AF imaging by confocal scanning laser ophthalmoscopy (cSLO)[18–21] or by fundus camera[22,23] allows visualization of the spatial distribution of fundus AF. In some retinal disorders, the distribution of fundus AF deviates from normal such that AF patterns can assist in diagnosis. Generally, differences in AF intensity within images have thus far not been comparable between patients, or even between successive images of the same patient. Notable exceptions are short-duration clinical,[18,24,25] and basic[26,27] studies of intensity in AF images obtained using the same cSLO and a comparative study of different cSLOs using an external fluorescence standard.[28]

Given the widespread use of fundus AF in clinical settings, there is a need for a standardized approach that can reliably determine AF levels at specific retinal locations so as to interpret fundus AF findings in relation to given pathologic conditions.[29] Some of the challenges associated with the quantification of AF from cSLO images have been discussed,[30] but no approach has been identified for clinical use.

AF quantification would aid in addressing questions such as whether a fundus area has normal or abnormal AF levels and whether AF levels correlate with disease progression. Thus, for Stargardt's disease, AF levels could provide valuable genotype–phenotype correlations, establish whether increased AF is indicative of an ABCA4 carrier state, and serve as potential metrics for response to therapy. For retinitis pigmentosa, AF levels in rings with high AF could be studied in relation to photoreceptor changes detected on spectral domain optical coherence tomography scans. For AMD one could determine whether higher AF in normal subjects is a risk factor for AMD. As treatments for these disorders become available, this approach could be used to monitor the efficacy of therapeutic interventions such as gene therapy or drugs designed to decrease RPE lipofuscin formation.

We have developed and tested a method to perform standardized quantitative measurements of fundus AF. This technique is applicable to SLOs and, in theory, to fundus cameras. The basic principle of the method is that when the AF from the fundus is normalized to the fluorescence of a standard

From [1]Schepens Eye Research Institute and the [2]Department of Ophthalmology, Harvard Medical School, Boston, Massachusetts; the Departments of [3]Ophthalmology and [5]Biomedical Engineering, Columbia University, New York, New York; and [4]Heidelberg Engineering GmbH, Heidelberg, Germany.

Supported by National Eye Institute Grants R01 EY015520 and R24 EY019861; the Foundation Fighting Blindness; New York Community Trust; and the Roger H. Johnson Fund, University of Washington, Seattle, WA.

Submitted for publication July 29, 2011; revised October 9, 2011; accepted October 10, 2011.

Disclosure: **F. Delori**, None; **J.P. Greenberg** , None; **R.L. Woods**, None; None; **J. Fischer**, Heidelberg Engineering (E); **T. Duncker**, None; **J. Sparrow**, None; **R.T. Smith**, None

Corresponding author: François Delori, Schepens Eye Research Institute, 20 Staniford Street, Boston. MA 02114; francois.delori@schepens.harvard.edu.

(mounted within the imaging device), the effects of variation in laser power and detector gain can be compensated. Thus, fundus AF can then be compared longitudinally, between eyes and between images obtained with different devices. In this article, we demonstrate how this approach can be implemented in two cSLOs. The underlying optical principles are presented in the Supplementary Material (http://www.iovs.org/lookup/suppl/doi:10.1167/iovs.11-8319/-/DCSupplemental). We have tested the method by comparing measurements between eyes, between sessions, and between instruments and by systematically varying common operator settings.

METHODS

Subjects

Thirty-four subjects (20 women and 14 men) with normal retinal status participated in the study. Twenty-four were white, and 10 were Asian, black, or of Hispanic ethnicity. Ages ranged from 20 to 55 years, and refractive errors from −4.4 to +3.7 D. All subjects had relatively good fixation and clear media, except for some floaters.

The tenets of the Declaration of Helsinki were followed, Institutional Review Board approval was granted, and informed consent was obtained for all subjects. The pupil of the test eye was dilated to at least 7 mm in diameter using 1% tropicamide and 2.5% phenylephrine. The retinal light exposures (recommended maximum power: 280 μW; 30° × 30° field; 488 nm) are below the limits recommended by the ANSI standards for durations up to 8 hours.[31,32]

cSLOs and Internal Reference

An HRA2 and a S3300 Spectralis HRA-OCT (both Heidelberg Engineering, Heidelberg, Germany) were used in this study (high-speed mode; 30° field; 768 × 768 pixels; 8.9 frames/s). With the exception of the internal reference, both devices were standard cSLOs with the excitation light (488 nm) generated by a laser (Sapphire; Coherent GmbH, Lübeck, Germany) and coupled via single-mode fiber into the camera head. The barrier filter in both devices transmitted light from 500 to 680 nm. The optical systems are similar as far as AF imaging is concerned (Appendix A, Supplementary Material, http://www.iovs.org/lookup/suppl/doi:10.1167/iovs.11-8319/-/DCSupplemental). Although the detectors were the same, the "advanced sensitivity mode" was used in the Spectralis, whereas this mode was not available for the HRA2. Consequently, the sensitivity settings of each device were different and not directly comparable. The laser power of the two cSLOs was monitored at intervals of 3 to 9 months and was always between 220 and 260 μW. It decreased by 0.4% to 1.4%/mo, probably varying with the use of the devices.

As the internal reference was mounted at the "intermediate" retinal plane of both cSLOs, it was always in focus with the fundus image (Fig. 1). Spectral and other characteristics of the fluorescent material are provided in Figure 2 and Table 1. An internal reference can also be readily inserted in a fundus camera as indicated in Appendix E, Supplementary Material (http://www.iovs.org/lookup/suppl/doi:10.1167/iovs.11-8319/-/DCSupplemental).

Image Acquisition

A single operator (JG) acquired AF images with both the HRA2 and the Spectralis. Room lights were dimmed (monitor glow only) to reduce possible effects on the test and to minimize distraction of the subjects. With the subject's head positioned in the chin-head-rest, the fundus was first aligned and focused with near-infrared light (820 nm). The 3-mm diameter scan pupil (intersection zone of the scanning laser beam; Appendix A, Supplementary Material, http://www.iovs.org/lookup/suppl/doi:10.1167/iovs.11-8319/-/DCSupplemental) must be located in the center of the subject's anatomic pupil by camera adjustments. The reflected and fluorescent lights from the fundus were captured in a 6-mm-diameter area in the pupil plane (detection pupil).

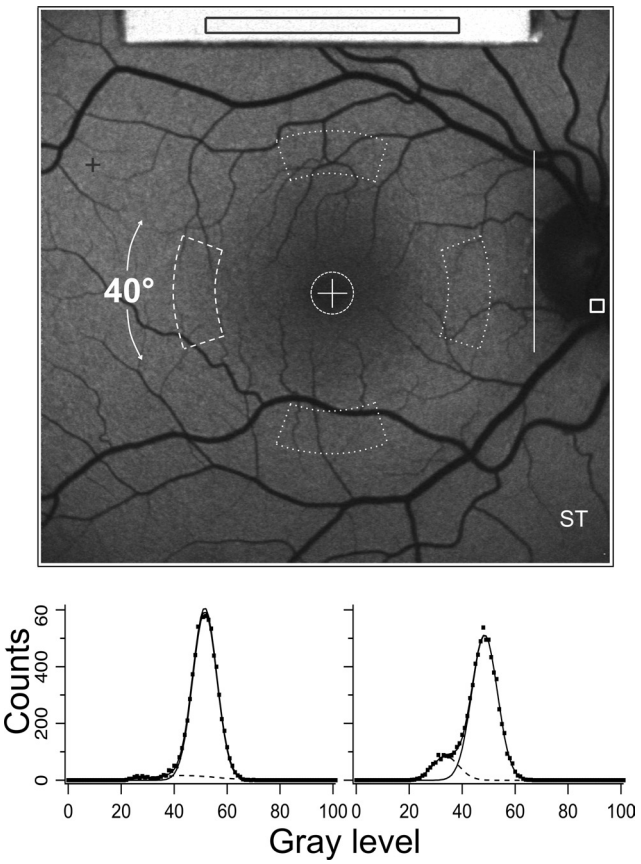

FIGURE 1. Autofluorescence fundus image from a 28-year-old man showing the internal fluorescence reference (*top*) that was recorded simultaneously with the fundus image. The average GL_R was always measured in the same rectangular area located over each reference. The protocol used for normal subjects consisted of calculating the mean GL in the different areas enclosed by *white dashed lines*. The analyzer positioned the *central cross* on the fovea and the *vertical line* on the temporal neuroretinal edge of the optic disc. The horizontal distance, L, between these landmarks served as a scale for the positions and sizes of all sampling areas; the foveal circle was 0.19 × L in diameter (≈2°), and the inside and outside radii of the four segments were 0.58 × L (≈6.6°) and 0.78 × L (≈8.9°), respectively. The angular width of each segment was 40°. For the emmetropic eye, the sampling areas were 2540 and 8030 pixels, for the fovea and for each segment, respectively. Highest (+) and lowest (*square*, on the optic disc) GLs were determined outside the contour of the reference. The highest level indicated whether the image GLs were within the range of linearity of the detection system. The lowest level was generally located on the optic disc. The histograms demonstrate how the influence of vessels is minimized: The sum of two Gaussians are fitted to the histogram, allowing the smaller Gaussian to account for the low GLs associated with the vessels while the large Gaussian accounts for the GLs in the fundus background. The center GL of the large Gaussian is then the mean level.

It was critical to centrally align the camera to avoid obstruction by the iris. The camera was aligned in all three dimensions such that optimal image uniformity was obtained (minimizing the extent of the lowest signals at the sides and corners of the image).

The laser was switched to the blue (488 nm) excitation mode, and the image was refocused until the whole field reached its maximum intensity. The focus was ≈1 D more myopic at 488 than at 830 nm, consistent with chromatic aberrations between the two wavelengths.[33] The sensitivity, S (acquisition screen: Sens.), was adjusted to avoid nonlinear effects (colored pixels appear in the image if GL is >252), followed by a bleaching period of 20 to 30 seconds to reduce photopigment absorption to <5%.[34–37] Final alignment of the camera

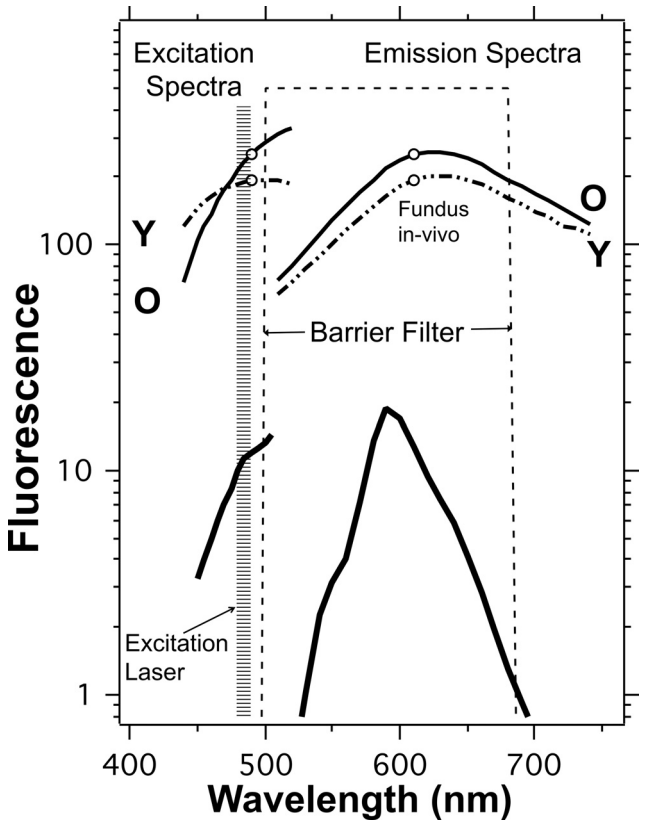

FIGURE 2. Excitation and emission spectra (*thick lines*, measured by spectrophotometry; MPF-44A; Perkin Elmer, Boston, MA) of the fluorescent material used in the study together with the spectral ranges of the excitation laser and of the barrier filter. Other characteristics of the internal reference are given in Table 1. For comparison, excitation and emission spectra of the fundus are shown for the 20- to 30-year age group (*dashed lines*, Y) and for the 60- to 70-year age group (*solid lines*, O). The spectra were measured by fluorometry,[14] with no correction for ocular media losses. The emission spectra between 500 and 535 nm were extrapolated. The excitation spectrum for older individuals is highly attenuated by the ocular media for wavelengths below 500 nm.

was made during that period. The patient was asked to blink a few times to provide a uniform tear film on the cornea. Eyelid interference, causing localized decreased signal, was avoided. Nine successive frames were then acquired. Frames were examined, and those demonstrating either localized (eyelid interference) or generalized (iris obstruction) decreased signal were eliminated (necessary in ≈10% of images). The frames were then aligned and averaged with the system software and saved in the nonnormalized mode (no histogram stretching), to create the AF image for analysis.

Image Analysis

To calculate the quantified (q)AF from gray level (GL) measurements in an image, we used:

$$qAF = RCF \times \frac{GL_F - GL_o}{GL_R - GL_o} \times \left(\frac{SF}{SF_{em,7.7}}\right)^2 \times \frac{\overline{T_{\lambda,20}} \times \overline{T_{\lambda,20}}}{\overline{T_\lambda} \times \overline{T_\lambda}} \qquad (1)$$

Details of the derivation of equation 1 are given in Appendix B and experimental verification of square law is described in Appendix C (Supplementary Material, http://www.iovs.org/lookup/suppl/doi:10.1167/iovs.11-8319/-/DCSupplemental). The parameters are:

RCF, reference calibration factor (see below)

GL_F, mean GL in the fundus area of interest

GL_R, mean GL in a defined area of the internal fluorescence reference (Fig. 1)

GL_0, zero signal level expressed in GL, provided by the system software ("offset" in "image info" panel). This signal is measured in raster lines outside the image, with the laser turned off and the detector on (images can be affected by room light).

SF, scaling factor in retinal micrometers per pixel (provided in image info). SF depends on the focus setting (refraction) and the corneal curvature of the subject (Appendix D, Supplementary Material, http://www.iovs.org/lookup/suppl/doi:10.1167/iovs.11-8319/-/DCSupplemental). SF can also be calculated from the Gullstrand-Emsley model eye.[33] $SF_{em,7.7}$ is the SF for an emmetropic eye with average dimensions.

$\overline{T_\lambda}$, $\overline{T_\lambda}$, Transmission of the ocular media at the excitation (Λ) and emission (λ) wavelengths, respectively. The transmissions $\overline{T_{\lambda,20}}$ and $\overline{T_{\lambda,20}}$ are the average transmissions for the media of 20-year-old subjects.

Thus, qAF represents the fundus autofluorescence relative to that which would be measured through the media of a 20-year-old emmetropic eye with average ocular dimensions.

The RCF was obtained, for each internal reference in each device, by in situ calibration with a (tentative) master reference, of the same fluorophore mounted 20 cm from the SLO's detection pupil (Table 1). The RCF for the HRA2 was 0.89 ± 0.04 that of the Spectralis, because the former was equipped with a slanted quarter-wave plate in front of the condenser lens (to reduce a reflection artifact), whereas the latter was not.

All AF images were analyzed with a dedicated image analysis program (IGOR, Lake Oswego, OR). The software transforms the entire image into a qAF-map of the fundus. Color-coded maps can also be generated, and they may be clinically useful. Average qAF can be computed in the preset regions (Fig. 1) or in manually selected areas of the image. In this study, we mainly analyzed the fovea, where AF is

TABLE 1. Characteristics of the Internal Reference

	Red Slide* + NDF† (1.3 DU)
Dimensions, mm	7 ×5 ×1.3
Peak emission, nm	590
Half-height points, nm	570–615
Change in excitation spectrum from 480 to 490 nm, %	+12
Fluorescence decay to 5% of peak, ns	29‡
Change in fluorescence after a 300-h exposure with 1.3 mW/cm² of 470–500-nm blue light, %	+0.8 ± 0.05§
RCF	
HRA2	260 (515)¶
Spectralis	231
Sampling Area	180 × 23 pixels

* Developed and tested for stability by Ping Chin Cheng (SUNY, Buffalo, NY). The fluorophore is Texas Red dye with other proprietary compounds embedded in a plastic matrix (Microscopy/Microscopy Education, McKinney, TX).

† Neutral-density filter (Wratten; Kodak, Rochester, NY) optically cemented to the slide. This method provides an attenuation of $10^{2\times1.3} = 398$, since both the excitation and emission are affected.

‡ The decay time must be short enough to ensure that sufficient fluorescence is detected before the horizontal scanner moves to neighboring areas (pixel clock: 100 ns in high-speed mode).

§ The test irradiance was 14× higher than the irradiance in the intermediate plane and 280× higher ($14 \times 10^{1.3}$) than the irradiance on the fluorescent material.

‖ An early version of the internal reference, used here in a few tests, used a lower NDF of 1.1 DU; the RCF was 515.

lowest, and the four segments, with emphasis on the temporal segment, where fundus AF is generally highest.[15]

We noticed that the focus readings necessary for best image quality in the same patients were different for the Spectralis and the HRA2 (Spectralis being 1.26 ± 0.26 D more myopic). The focus readings for the HRA2 agreed with the refractive error determined by autorefraction (Nidek, Hiroishi, Japan). Therefore, we corrected the Spectralis' focus by adding 1.26 D. This decreased SF, thereby reducing qAF by 3% to 4% (Appendix D, Supplementary Material, http://www.iovs.org/lookup/suppl/doi:10.1167/iovs.11-8319/-/DCSupplemental). We also found that the zero GL_0 given by the software (offset) was 0.6 to 0.8 GLs ($P < 0.001$) higher than that measured in a completely dark room. This small error will only affect qAF when a very low AF is measured.

In the present study, we did not measure individual corneal curvatures (needed for computation of SF; Appendix D, Supplementary Material, http://www.iovs.org/lookup/suppl/doi:10.1167/iovs.11-8319/-/DCSupplemental) but used the default value of 7.7 mm. Also, we did not, at this point, individually correct qAF for losses of light in the ocular media.

Statistical Analyses

Since sample sizes were generally small, we used nonparametric statistical tests (performed with StatPlus; AnalystSoft, Vancouver, BC, Canada, and SPSS 19.0 for Mac; SPSS IBM, Chicago, IL). To measure test–retest repeatability and between-instrument agreement between two measures qAF_1 and qAF_2 ($\Delta qAF = qAF_2 - qAF_1$), we used the widely accepted method of Bland and Altmann.[38] Since stepwise regression showed a weak positive association between the absolute values of ΔqAF and qAF (consistent with a component of the measurement noise being related to signal strength), we transformed ΔqAF into the relative values $\Delta qAF/\overline{qAF}$. The (coefficient of) repeatability, expressed in percent, is then:

$$\text{Repeatability} = \pm 1.96 \times \sigma_{\Delta qAF/\overline{qAF}} \times 100 \quad (2)$$

This equation provides the 95% confidence intervals for testing under the same conditions (e.g., same day, different days). In this article, we use the term *repeatability* for comparisons within instrument. *Agreement* is also defined by equation 2 and was used when the two instruments were compared. Repeatability is the coefficient of variation in percent, multiplied by 1.96. If the variability of measurements increases (increased measurement noise), so will the repeatability (interval).

Results

To illustrate the main features of the method and its ability to account for changes in detector gain, G, we analyzed images from an eye over a range of Ss (Fig. 3). S denotes the setting on the control panel, whereas gain G denotes the actual relative gain of the detector. The GLs of the fundus and the reference increase with S, corresponding to the change in G. The quantified autofluorescence, qAF (equation 1), was independent of S despite an increase in G by a factor 2.1 (S = 89–93). Small variations in qAF were probably due to instrument noise, subject fixation, and other sources of measurement noise.

Linearity

For equation 1 to be applicable, the GL output of the detection system must be linear with respect to the intensity of the actual fluorescent signal. To test the linearity of the HRA2 and the Spectralis, we imaged a pattern located 20 cm from the detection pupil of the camera (focus, 5 D). It consisted of a raster with 36 calibrated fluorescence intensities (Fig. 4, inset). Images of the pattern were recorded at different S for the two cSLOs, and the results were adjusted to simulate an equal laser power for both devices. The two devices were linear for exposures that produced $GL < 175$ (Fig. 4). At higher exposures, the fluorescence was increasingly underestimated. Although none of the pixels of the mean image reached a *GL* of 255, some pixels in the nine individual frames did, causing the mean to deviate from linearity.

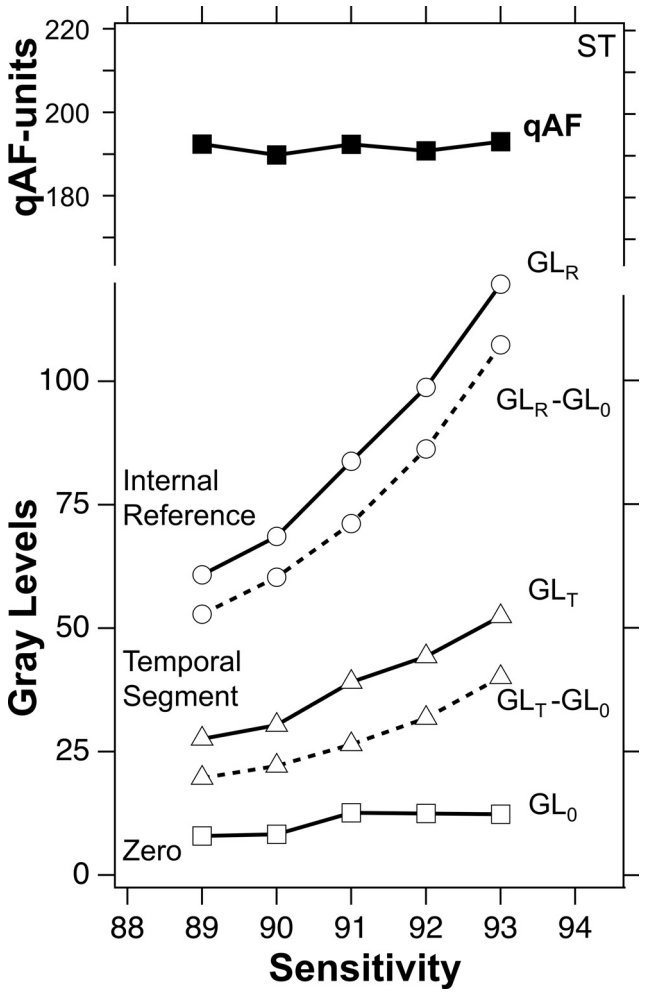

Figure 3. Gray levels (*solid lines*) for the temporal segment (△), the internal reference (○), and the equivalent zero GL_0 (□) as a function of sensitivity for images from the subject in Figure 1. qAF (■) was derived from equation 1 by substitution of $GL_T - GL_0$ and $GL_R - GL_0$ (*dashed lines*, corrected for GL_0), the reference calibration factor RCF = 515 (HRA2, Table 1), and the scaling factor SF = 11.38 μm/pixel for the tested subject. The zero GL_0 is shifted electronically to remain at 10 to 14 GLs. Despite an increase in the mean GLs by a factor 2.1, the qAF changed only slightly (coefficient of variation = 3.3%).

Bleaching before qAF Imaging

To verify whether the 20-second bleaching period before AF imaging was sufficient to adequately reduce the absorption of photopigment, we recorded, in three subjects, the decrease in attenuation during bleaching (Fig. 5). Although there was a surprising lack of variability among these subjects, the bleaching duration of 20 seconds appeared adequate for rods. Longer bleaching exposure may be needed for older subjects. For foveal cones, a slight increase in attenuation was observed after 30 seconds of bleaching (Fig. 5).

Quantitative AF at Different Sensitivities

To assess the efficacy of the internal reference approach at accounting for different laser powers and sensitivities (S), we

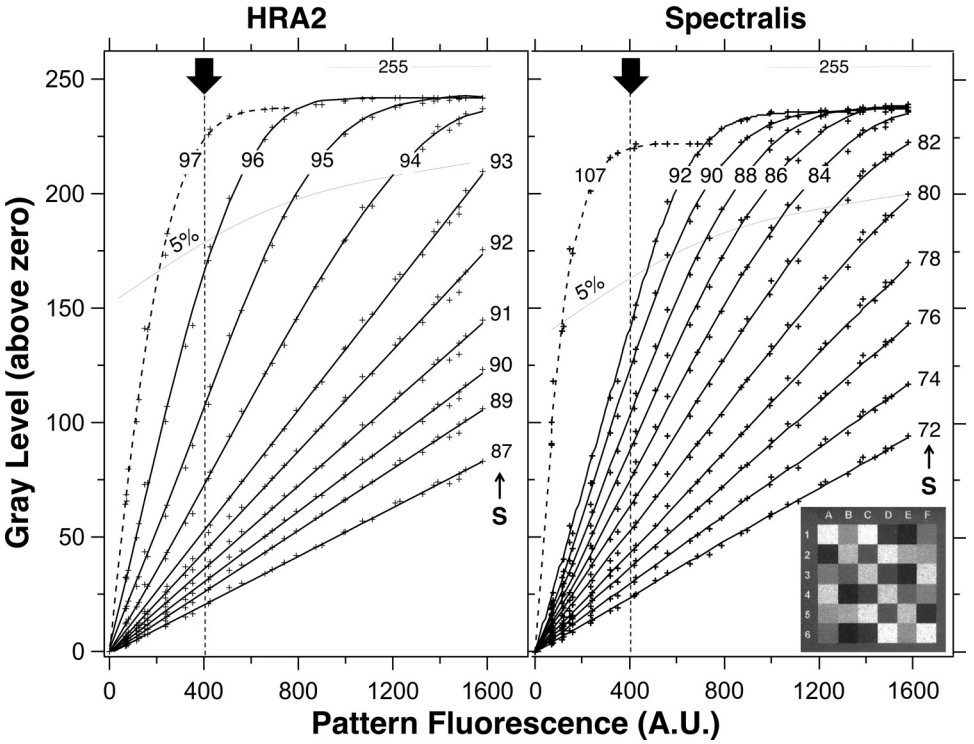

FIGURE 4. Zero-corrected gray levels (GLs) versus the fluorescence of a calibrated pattern $AF_{pattern}$ at different sensitivities, S, (as indicated) for the HRA2 and the Spectralis. *Inset*: an image of the calibrated pattern. *Dashed lines*: point at which nonlinearity reached 5% at different sensitivities. Pixel-sized flashes of colored light appear slightly below the 5% level. For high exposures, the GLs saturate at a level of $255 - GL_0$. The range of $AF_{pattern}$ was chosen to correspond roughly with measurements previously obtained by fluorometry: normal subjects ($AF_{pattern}$ = 200–400), patients with AMD ($AF_{pattern}$ = 300–500), Stargardt's disease ($AF_{pattern}$ = 500–1200), and Best disease ($AF_{pattern} \approx 1600$).[1,13–15] *Dark arrow*: the equivalent exposure for the internal reference currently used in the study. For example and for the HRA2, if we set a lower limit for $GL - GL_0$ to 25 (mainly for contrast), then the reference should be adequate to cover a large range of fundus AF levels ranging from an equivalent of 1600 (using S = 89, $GL_F - GL_0 \approx 110$, and $GL_R - GL_0 \approx 25$ at the limit) to an equivalent of 100 (using S = 96, $GL_F - GL_0 \approx 25$ at the limit, and $GL_R - GL_0 = 165$).

recorded (as we did in Fig. 3) single images obtained at different Ss from the fundi of eight subjects (age range, 21–35 years) and from three stationary fluorescent targets A, B, and C. The target tests were repeated three times (Fig. 6).

The qAFs (normalized to one S) at the two retinal sites correlated significantly (Spearman $\rho_{39} = 0.40$; $P = 0.01$), indicating that the qAF changes are due in part to factors that affected the entire image (e.g., obstruction by the iris, tear film alterations). This similarity is apparent in Figure 6 for some subjects (e.g., KD and TY), in the variation of qAF with S for the temporal and foveal sites.

All data were analyzed for the influence of S in the same range of detector gains (HRA2, S = 89–93; Spectralis, S = 72–84). In the eight subjects, the temporal measure had a higher qAF than did the foveal (repeated-measures ANOVA, $F_{1,7} = 39.4$; $P < 0.001$), and there was no effect of S on qAF ($F_{4,28} = 0.78$; $P = 0.55$) at both retinal sites (i.e., no interaction, $F_{4,28} = 0.95$; $P = 0.45$). For the data on the three stationary fluorescent targets, there were large differences in qAFs between the targets (Greenhouse-Geisser corrected $P < 0.001$), but no effect of sensitivity ($P > 0.14$).

It is apparent from Figure 6 (logarithmic plot) that the measurement noise increased with decreasing qAF for both subject and pattern data (see also later discussion). Furthermore, the noise was higher for the subject data because of errors related mainly to changes in alignment and head/eye movements.

Similar tests were performed on the stationary fluorescent target by adjusting the laser power from 210 to 250 μW. No differences in qAF were detected (four sites, two sensitivities each; Wilcoxon $Z_7 < 0.4$, $P > 0.7$).

Field Uniformity

We assessed the field uniformity of the fundus excitation and AF detection by acquiring five to eight fundus images in each of five subjects using different fixations provided by the HRA2 as well as some intermediate fixation positions (Figs. 7A, 7B). Uniformity profiles were obtained by plotting the qAF relative to that at the image center as a function of eccentricity (Fig. 7C). Although some small asymmetries (e.g., top-bottom or left-right) were detected in individual subjects, we assumed that the profiles were circularly symmetric.

The uniformity profiles all show a decreasing signal with increasing eccentricity: at an eccentricity of 10°, the qAF was ≈95% of the central value, and it decreased further to ≈85% at the edge of the field (eccentricity, 15°). The corners of the image were always the darkest (60%–80%). Thus, the area of highest uniformity was a 20°-diameter circle centered in the field, where average signals did not drop below 95%. Nonuniformities are caused by the optics between the intermediate plane and the retina (camera lens and ocular optics), because uniformity was observed in the intermediate plane (Fig. 7C, bottom profile).

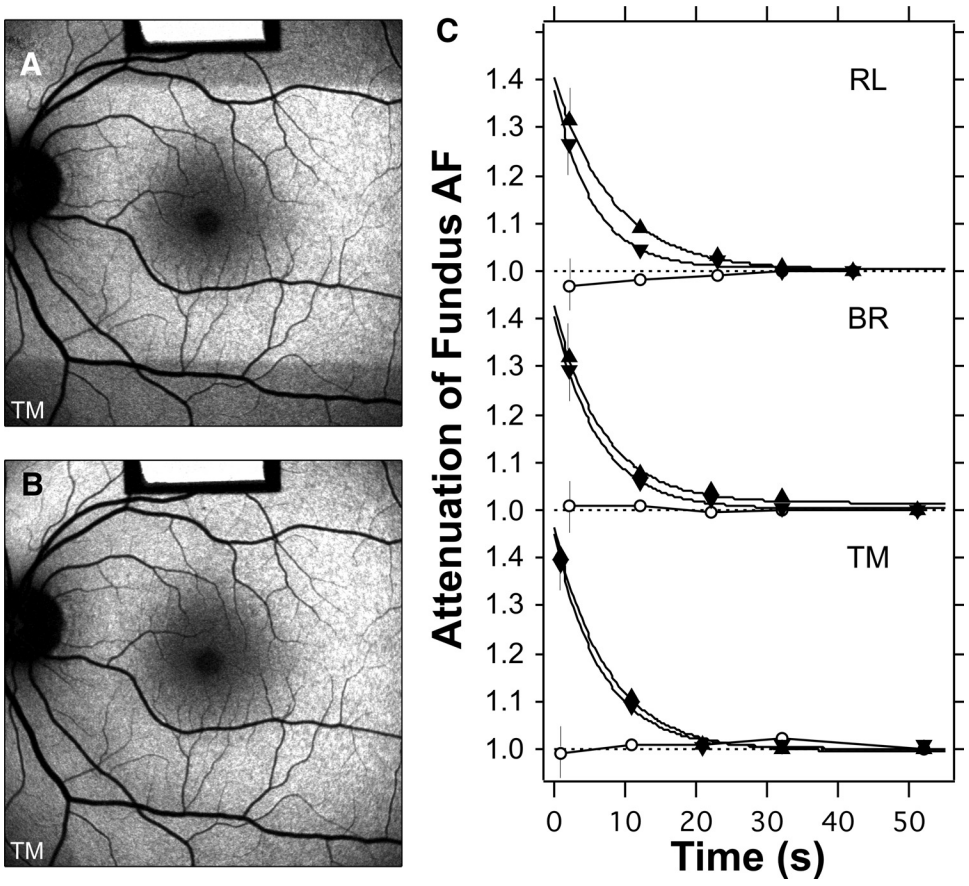

FIGURE 5. Bleaching of photoreceptors, using the 488-nm illumination with laser power of 260 μW through the pupil. The test started with a 30-second exposure using the 20° field (images not recorded). The irradiated area was then 20° × 30°, or 0.53 cm^2, and the retinal irradiance was 490 μW/cm^2. The rods in the 20° high strip were then bleached to 99%; no changes in AF were detected in the subsequent images. (**A**) A 30° fundus image was taken immediately after the field was switched to 30° × 30° (0.79 cm^2).The retinal irradiance was then 330 μW/cm^2. The superior and inferior fundus was then roughly dark adapted. Images were recorded after 11, 21, 31, and 51 seconds, to document the effect of bleaching. (**B**) Image recorded 30 seconds after image (**A**). No clear differential AF was detected between the areas that were and were not initially bleached. (**C**) Time course of the attenuation of the AF during bleaching for three subjects (age range, 23–47years). Error bars are SD, calculated from propagation of errors. Measurements were made within the superior (△) and inferior (▽) dark bands, at the boundary of the dark area (eccentricities, 12°–17°), and in the fovea (○). The AF measured in the bleached zone outside the fovea acted as the reference. The data were fitted by exponential functions. At $t = 0$ the attenuations ranged from 1.37 to 1.47, corresponding to optical densities of 0.16 to 0.19 DU for the rods (500 nm). The attenuation was reduced to 1.05 (5% absorption) after a bleaching duration of 12 to 17 seconds and to 1.02 (2% absorption) after 17 to 24 seconds. Marginal increases in AF were observed at the fovea for RL and TM (○), perhaps related to regeneration of the photopigment.

Repeatability

Repeated analysis of the same image yielded repeatability of ±1% to ±1.5%, reflecting positioning of the sampling areas.

We tested repeatability of qAF in both eyes of 12 subjects (ages, 25–50 years) using both the HRA2 (S = 91–94) and the Spectralis (S = 72–90). In addition to the fovea and the temporal segment, we also considered the larger sampling area of all four segments (Fig. 1). We tested repeatability for qAFs obtained from images (1) within a session (sitting), (2) between sessions on the same day, and (3) between sessions on different days (Fig. 8). No statistically significant differences were found between those repeated measures at any site, except as mentioned below.

Within Session. Two successive images were obtained within a session (≈2–6 seconds apart) using the same positioning in the chin/head rest, alignment of the camera, and focus. Different sensitivities were used, but they were the same for each image pair. Repeatability was ±6.9% for the fovea and improved to ±2.7% for the four-segments (Fig. 8). As repeatability is a 95% confidence interval, a subsequent foveal qAF measurement taken within a session will only differ from the first measurement by more than 6.9% on 5% of occasions.

Between-Sessions, Same-Day. For qAF data obtained in two sessions on the same day (<5 minutes apart), the operator selected the same sensitivity in 58% of the cases. Having the subject move away from the instrument made the qAF measurements more variable than those within session, as repeatability was ±6% to ±11% at the three sites (Fig. 8). For the fovea, the qAF for the second session was slightly smaller than that in the first (by ≈2%; Wilcoxon $Z_{31} = 2.0$, $P = 0.05$). Since this effect on qAF appears to be exacerbated by low fundus AF, we speculate that the determination of the GL_0 level may be responsible. This possibility is being investigated further.

Between Sessions Different Day. For qAF data obtained on different days (28–64 days apart), the same S was selected in 33% of the cases. Repeatability was ±7% to ±14% (Fig. 8), slightly worse than the same-day measurements, suggesting that much of the difference in repeatability between within-session, same-day and between-sessions was due to subject alignment and related issues.

The differences (ΔqAFs) at the foveal and temporal segments correlated with each other for both the within-session (Spearman, $\rho_{70} = +0.41$; $P = 0.0007$) and the same-day, between-session comparisons ($\rho_{30} = +0.61$; $P = 0.0002$). Furthermore, significant correlations were found between the ΔqAFs for the other sites (nasal, superior, and inferior segments; data not shown). In fact, 32% (within-session) and 47% (same-day, between-session) of all comparisons showed either an increase or a decrease in qAF at all five sites, although the differences were not uniformly distributed.

Internal Reference. The $GL_R - GL_0$ normalization term was used in equation 1 to account for variations in laser power, gain, and other sources of instrument noise, but can also be used to characterize measurement noise from the instrument alone under the above conditions (as shown in Fig. 8). Repeatability of $GL_R - GL_0$ is derived from images obtained at the same S. Within-session repeatability for $GL_R - GL_0$, was ±1.2% and ±2.0% for the HRA2 and the Spectralis, respectively (n =

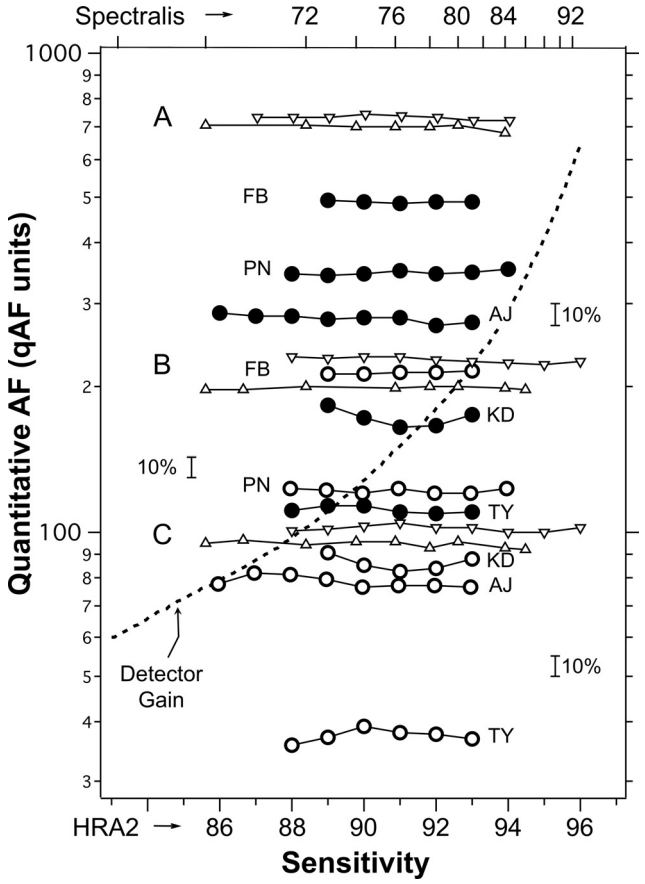

FIGURE 6. Relative stability of qAF measurements obtained from images recorded with different sensitivities in five subjects (initials) by the HRA2 (temporal segment, ●; fovea, ○), and for three targets A, B, and C from stationary fluorescent patterns using the HRA2 (▽) and the Spectralis (△, sensitivity top scale). Some curves were displaced vertically to avoid overlap. Small brackets indicate a change of 10%. If no internal reference were used to obtain qAF, then all data would vary approximately as much as the variation of the detector gain (*dashed line*). The relationship of the sensitivities of the two devices, implied by the *top* and *bottom* axes is valid only for the study cSLOs. The exact relationship could vary from instrument to instrument, particularly at high gain.

66 and $n = 67$). Between-session, same-day repeatability was ±3.1% and ±4.2% for the HRA2 and the Spectralis, respectively ($n = 21$ and 4; Spectralis has many more S settings than HRA2, and thus few pairs with the same S). The GL_R of the internal reference was lower for the second session than the first (by 2% ± 1%; Wilcoxon $Z_{17} = 3.3$, $P = 0.0009$), and that seems to be related to the decrease in foveal qAF sessions conducted on the same day, as reported above.

Between-session, different-day repeatability (over a 4-month period) was ±4.7% and ±5.7% for the HRA2 and Spectralis, respectively ($n = 95$ and 89), but this was complicated by the variability in between-session durations and gradual reduction in the GL_R over time (a systematic bias for each device, Spearman $\rho_{142} = -0.35$; $P < 0.0001$), presumably due a reduction in laser power. Internal reference repeatability indicates the lower limit on the repeatability that is possible with these two cSLOs, as configured (i.e., if subject-related sources of error could be minimized). As described next, those limits will also vary with the sampling area and qAF.

Effects of Sampling Area and qAF Level. Figure 8 shows that repeatability for the fovea was worse than for the temporal segment, which was worse than the four-segments. To evaluate the effects of sampling area and qAF level on measurement noise, we estimated within-session repeatability with smaller sampling areas for subjects and for stationary AF patterns (Table 2). Repeatability was worse as qAF decreased (multiple regression, $t = 5.2$; $P < 0.001$) and as sampling area decreased

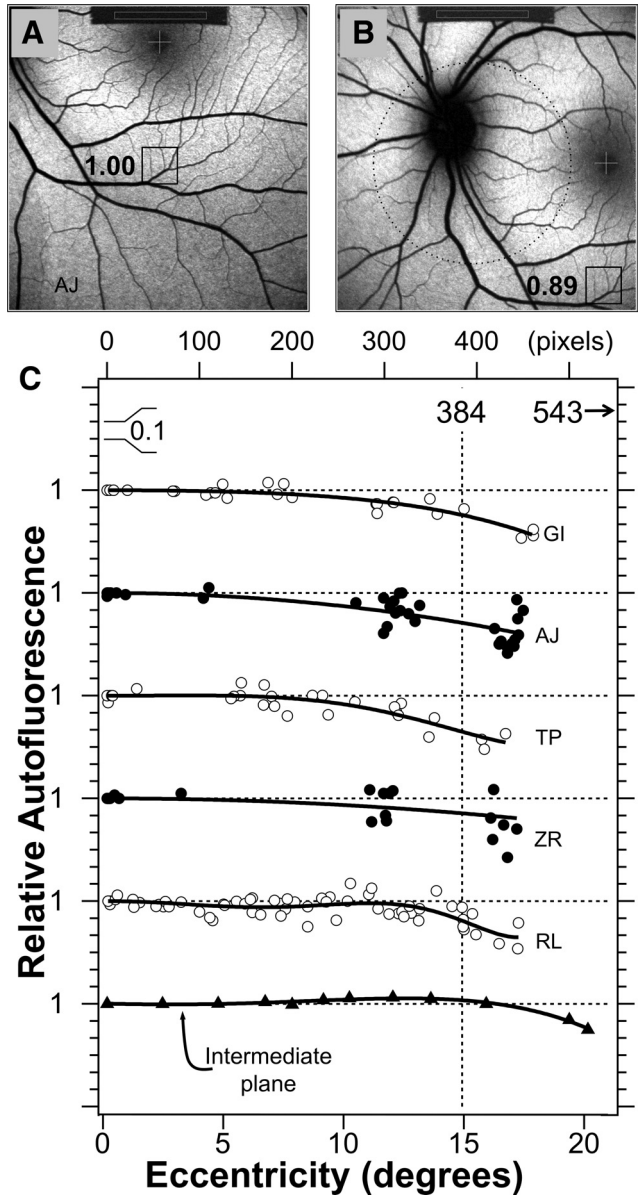

FIGURE 7. Testing the uniformity of qAF images. Images for an inferior (**A**) and nasal (**B**) fixation. The boxed areas correspond with the same fundus areas (100 × 100 pixels) located at a fixed horizontal and vertical offset from the center of the fovea. The numbers are the ratios of the mean GL in that area to the mean GL in the same area when it is located in the center of the field. Such comparison was repeated 15 to 30 times for different fundus sites and fixation positions. *Dotted circle*: a 20°-diameter area centered in the field. (**C**) Relative AF for five subjects as a function of eccentricity. The bottom profile was measured in the intermediate plane of the HRA2 by placing a uniformly fluorescent material in that plane. Profiles were displaced for clarity; each *horizontal dashed line* corresponds to a ratio of 1 for the profile below it (0.1/division). *Vertical dashed line*: the eccentricity of 768/2 = 384 pixels (15°) and the corners of the image have an eccentricity of 543 pixels (23°). The smooth lines are sixth-degree polynomials that were fitted through the data (even terms only, offset = 1). The mean relative AFs (±SD) at 10° and 15° eccentricity were 0.95 ± 0.03 and 0.84 ± 0.05, respectively.

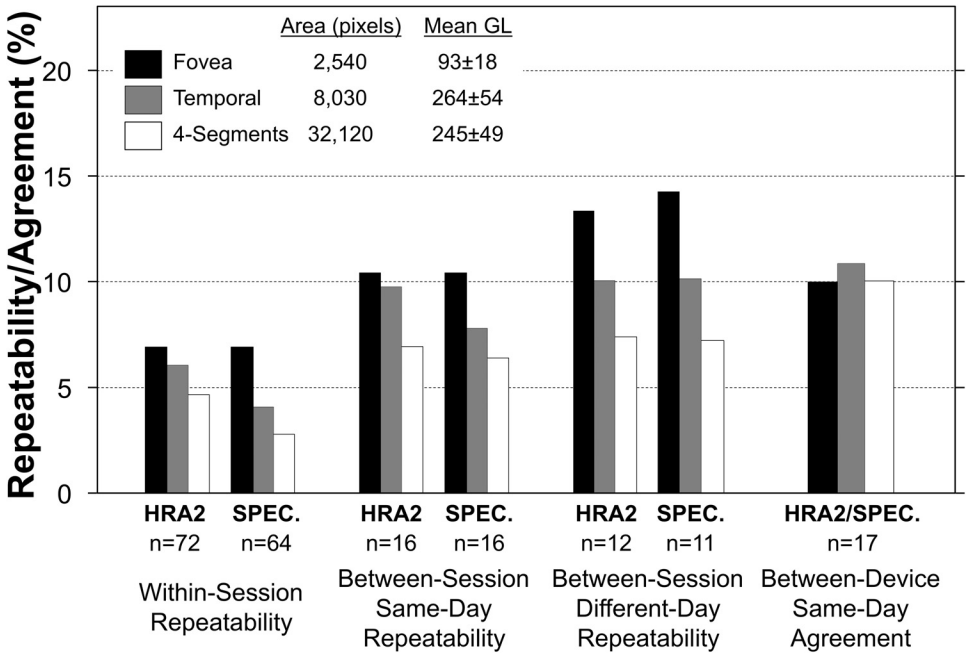

Figure 8. *Repeatability* (equation 2) of qAF measurements obtained from two images within a session, from two sessions on the same day (<5 minutes apart), and from two sessions on different days (28–64 days apart), and *agreement* (equation 2) between qAF measurements on the HRA2 and the Spectralis on the same day. Repeatability was better (smaller) within sessions than between sessions, suggesting that positioning of the subject's eye is a major source of measurement noise. Repeatability had the same pattern for all comparisons, improving with increasing sampling area and increasing fundus AF. The two cSLOs had similar repeatability (no significant differences between ΔqAF distributions, Kolmogorov-Smirnov two-sample; $P \geq 0.08$). In one session, three to four images were acquired, separated by blinking and, if necessary, minor realignment of the camera. For between-session and between-instrument comparisons, two images from each session (randomly selected from session images) were averaged to provide the data. Repeatability and agreement computations included corrections for the use of multiple measurements per session.[38] Test–retest measurements were made in 12 subjects, 10 of whom had both eyes tested. As there were no significant correlations between the differences, ΔqAF, obtained from left and right eyes (three comparisons: $\rho < 0.3$; $P > 0.26$) data for both eyes were used.

($t = 7.0$; $P < 0.001$). The effect of area was stronger for fundus images than for patterns ($t = 2.65$; $P = 0.016$). On average, repeatability for the fundus images was 2.4 times worse than that for patterns ($t = 10.0$; $P < 0.001$).

Between-Instrument Agreement

qAF in 17 eyes (nine subjects; ages, 25–50 years) measured with the HRA2 (S = 91–94) was compared to that measured with the Spectralis (S = 72–90) on the same day. qAFs measured with the Spectralis exhibited a tendency to be lower than those measured with the HRA2 at the fovea (by 2% ± 4%; Wilcoxon $Z_{16} = 1.8$, $P = 0.08$) but no differences were detected for the temporal segment (Wilcoxon $Z_{16} = 1.0$, $P = 0.3$) or the four-segments (Wilcoxon $Z_{16} = 0.8$, $P = 0.4$). After correction for the Spectralis focus (the Methods section), the absolute difference in the foci of both devices was 0.17 D (IRQ = 0.21 D).The agreements (between the HRA2 and the Spectralis) were <11% (Fig. 8), but did not show the benefit of larger area sampling observed in the repeatability tests. We suspect that this was due to asymmetrical nonuniformities caused by slight misalignment of one of the devices.

Table 2. Within-Session Repeatability of qAF for Different Sampling Areas

Site (Eccentricity)	Image Pairs (*n*)	Sampling Area* (Pixels²)	Mean gAF (qAF Units)	Repeatability† (%)
Fundus Sites				
Mean of four-segments‡	115	32,120	240	3.5
Segments (6.6–8.9°)‡	115	8,030	220–250	3.9–4.7
Superotemporal (13°)	23	830	290	5.1
Inferior to fovea (1°)	23	850	140	5.9
Fovea (2° diam. circle)‡	115	2,540	90	6.3
Superior (10°)	23	140	260	6.4
Fovea (1.4° diam. circle)	23	1,270	80	7.2
Temporal (13°)	23	480	225	7.3
AF Targets§				
Master Reference	15	14,000	460	0.6
Internal Reference	70	4,140	230–260	1.4
Target B	15	7,300	220	1.6
Target C	15	2,050	90	3.1
Cell B3, Pattern (Fig. 4)	20	130	190	4.4

* One optic disc area in a 768 × 768 image is ≈10,000 pixels².

† Repeatability for image pairs obtained using the HRA2 and the Spectralis (Heidelberg Engineering, Heidelberg, Germany).

‡ Same sites as those in Figure 8.

§ Representative data from stationary AF pattern (of a total of 15 pairs).

Effects of Errors in Focus and Alignment

We investigated how focus errors and changes in axial and lateral position of the cSLO with respect to the eye contributed to these measurement errors. Deviation from the focus that gave maximum AF intensity (the end point in AF imaging) by ±0.6 D resulted in a 5% decrease in qAF (Fig. 9A). Thus, it is unlikely that this error in focus played a major role, since the absolute difference in focus between sessions was only 0.20 D (IRQ = 0.31 D, same day) and 0.27 D (IRQ = 0.28 D, between days). Axial movement of the camera (Fig. 9B, left) produced drastic darkening of the corners but less than a 5% change in qAF in the range of foci expected from an experienced operator. Uniformity in the image did not change by more than 5%. Lateral displacement (Fig. 9B, right) also resulted in a less than 5% change in qAF, so long as the iris did not obstruct the detection pupil. This resulted in a rapid and initially generalized decrease in qAF, eventually accompanied by substantial changes in uniformity. Each of these factors demonstrated a combination of uniform qAF changes and some nonuniformity.

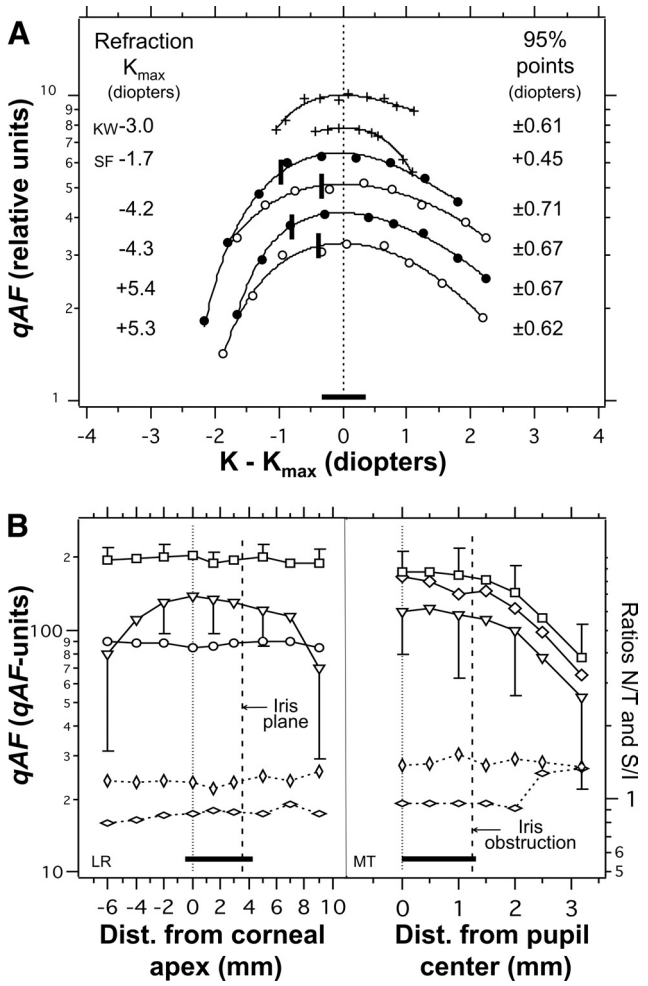

FIGURE 9. Variations in qAF resulting from errors in focus and alignment. *Horizontal bars*: ranges applicable to a skilled operator. (**A**) Relative qAF versus the difference between the focus K and the focus yielding maximum AF (K_{max}) for two subjects (+), with the Spectralis, and for a stationary fluorescent pattern (with resolution target), with the Spectralis (○) and the HRA2 (●). Each curve is normalized to its maximum qAF (0 D). The curves were displaced to avoid overlap. The 95% points indicate the focus change at which qAF decreased to 95% of the maximum. *Solid vertical bars*: the focus position that yielded maximum sharpness (modulation) of the resolution pattern (10 pixels/line pair). This occurs at a slightly more myopic focus than that which produces maximum AF intensity (which is generally the focus obtained by operators). (**B**) *Left*: Changes in qAF with axial distance between the scan pupil (incident laser beam) and the corneal apex (±0.5 mm accuracy). Data are shown for the fovea (○), the mean of the four-segments (□), and the mean of the four corners of the image (▽; 75 × 75 pixels in each corner). (**B**, *right*): Changes in qAF with lateral distance between the center of the scan pupil and the center of an 8.5-mm dilated pupil. External fixation was used, resulting in an 8° more nasal fixation. qAF measurements were from the image center at roughly midway between the disc and fovea (◇), from four-segments located at 12° from the image center (□; more eccentric than in Fig. 1: nasal to the disc and temporal to the fovea), and from the image corners (▽). (**B**, *left* and *right*) Bottom plots represent the ratios of qAFs (*right*) measured in the temporal and nasal segments (T/N, *horizontal lozenges*) and in the superior and inferior segments (S/I, *vertical lozenges*). Changes in these ratios reflect changes in uniformity; the axial and lateral displacements did not result in changes larger than 5%.

qAF as a Function of Age

qAF exhibited a significant increase with age both at the fovea and in the four-segments (Fig. 10), even without correction for ocular media absorption. All subjects were white and had normal retinas (n = 20, 20–50 years). The measurements were made over a 6-month period with the two cSLOs. The correlation for the fovea was less significant than that at the temporal site because foveal AF is variably attenuated by macular pigment absorption. When corrected for ocular media absorption using an algorithm[39] that predicts the optical density of the media at a given age and wavelength (Appendix F, Supplementary Material, http://www.iovs.org/lookup/suppl/doi:10.1167/iovs.11-8319/-/DCSupplemental), the rate of increase in the four-segment qAF was 8.6 qAF units/y, slightly smaller than an equivalent rate of 12 qAF units/y found by fluorometry in a much larger population.[15]

DISCUSSION

Measurement of AF from images obtained using SLOs and fundus cameras is feasible if images of high quality and uniformity are recorded by a skilled operator,[40] if care is taken to adjust exposures within the range of linearity (Fig. 4), and if the important retinal features are aligned within the central 20°-diameter circle with the highest uniformity (Fig. 7). Additional requirements include bleaching the photopigment (Fig. 5) and recording multiple images in one test session to ascertain individual variability. The advantages of the internal reference approach were demonstrated by the relative resistance of qAF to changes in S and laser power (Fig. 6), and by the fact that measurements taken at protracted time intervals and on different devices were reproduced with reasonable accuracy (Fig. 8). Therefore, qAF measurements using the established protocols can be performed in clinical settings and can be exchanged between investigators. Even though these advantages would be forfeited if an internal reference were not used, that does not preclude conducting valuable quantitative studies without an internal reference, as long as they are performed using the same instrument over a short time period. The benefit of using an internal reference in such studies will depend on the instrument-related noise (repeatability of ±3% to ±6% between sessions for our instruments), systematic errors (as noted above), and the effect magnitude and time interval being studied.

Limitations of our study include the difficulty of identifying technical issues and adapting protocols; recording of all images by a single operator to avoid interoperator variability during these initial studies; and the testing of only young subjects (≤55 years) with reasonably good fixation. Furthermore, the presence of the internal reference in the image compromised the software alignment of the frames, particularly when fixation was poor (the stationary reference and the moving fundus image compete for alignment). This resulted in the blurring of the reference image and/or suboptimal alignment of the fundus features. Heidelberg Engineering has now developed modified software that aligns the fundus image but not the area occupied by the reference. This modification could also be implemented in the software of the ART (automatic real-time averaging) mode. The ART-mode, in which frames are continuously aligned and averaged into one image, was not used in this study because it did not allow for examination of individual frames and the manual rejection of degraded frames (decreased signal, distortions due to movement) before calculating the mean image. The ART software currently rejects distorted frames but could be modified to include a rejection algorithm dealing with partially obscured frames.

Internal Reference

The requirements for the ideal fluorescence reference material are an efficiency that is close to that of fundus AF measured at the intermediate plane, an emission spectrum matching the

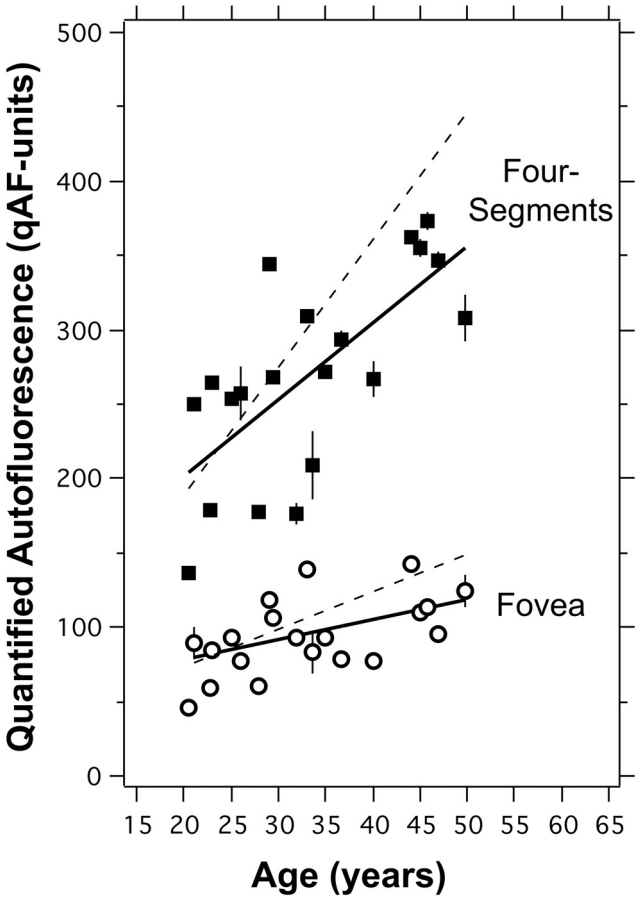

FIGURE 10. qAF versus age for 20 subjects (age range, 20–50 year, all white) for the average of the four-segments (■) and for the fovea (○). Error bars are ±1 SD. Linear regression lines through the data showed a significant increase in qAF with age. For the four-segments, qAF = 201 + 5.22 × (age-20) (r_{19} = 0.70; P = 0.0005), and for the fovea, qAF = 76 + 1.35 × (age-20) (r_{18} = 0.52; P = 0.02). *Dashed line*: regression lines for the data (symbols omitted for clarity) of the four-segments and foveal sites after accounting for media absorption with the algorithm of van de Kraats and van Norren[39] (Appendix F, Supplementary Material, http://www.iovs.org/lookup/suppl/doi:10.1167/iovs.11-8319/-/DCSupplemental); the rate of increase of qAF with age was then 8.6 and 2.7 qAF units/year for the four-segments and fovea, respectively.

emission spectrum of fundus AF (Fig. 2), an excitation spectrum that is relatively flat from 480 to 490 nm (the latest Spectralis uses laser diodes with central wavelength in the 483–488 nm range), photostability, insensitivity to temperature changes, and availability in thin (1 mm) glass or plastic plates. Clearly a compromise was needed.

The fluorescent material was selected from seven commercially available materials that we tested extensively. For this internal reference, we succeeded in matching its peak emission (590 nm) with that of fundus AF (~590–630 nm); however the spectral width of the material was narrower than that of the fundus AF (Fig. 2). Roughly matching the complete emission spectra of the reference with that of the fundus may be a difficult task, as most inorganic fluorophores have much narrower emission spectra and few extend above 600 nm. The stability test that we performed addressed only light exposure, not the shelf stability of the fluorophores. In any case, each device will require calibration with an external master reference to account for differences in internal references and the optics of the device. The master reference used in this study was an expedient and economic, but not long-term, solution. We plan to use an available fluorescence reference with very stable characteristics (Avian Technologies, New London, NH). We anticipate that manufacturers and service personnel will use that master reference, mounted so that it can be installed on different devices, to calibrate each device.

The choice of the efficiency of the internal reference is critical. It should be such that, at the highest sensitivity routinely used with the camera (96 for HRA2, 92 for Spectralis), the GL of the internal reference should be high but not exceed the limit of linearity (Fig. 4), thus allowing imaging of the full range of retinal AF intensities. However, if higher sensitivities are needed (e.g., in mouse studies), a less efficient internal reference should be used (different NDF, Table 1).

qAF units are arbitrary units. However, since the average qAF for a 20-year-old subject with normal retinal status was found to be ≈200 qAF units, we felt that this may be a reasonable way to define the qAF unit.

Measurement Noise

Measurement errors associated with in vivo qAF determinations were more important than the influence of statistical noise of the AF signal and digitization electronics. This finding is evident from the near tripling of repeatability for within-session tests (within 6 seconds) on a stationary pattern, compared with that measured in subjects (Table 2) and from the near doubling of repeatability for within-session compared to between-session, same-day qAF of subjects (Fig. 8). In this regard, it is unlikely that the use of 16 frames/image, instead of the 9 frames/image used in this study, would substantially improve repeatability, since it would reduce only (by 33%) the relatively small statistical noise.

The positive correlation between the ΔqAFs at different sites and the large percentage (30%–50%) of image pairs where the qAFs of all sites either increase or decrease, albeit not uniformly, suggest that common effects in the anterior eye are responsible for these errors. Such effects may be changes in the tear film, in focus, and in the axial and lateral alignment of the camera with the eye. Although errors in focus appear to be a minor possibility, axial and lateral adjustment of the camera results in a ±5% change in qAF over ranges applicable to a skilled operator. However, asymmetries are also frequently observed, possibly due to asymmetries in the optical elements of the eye, to differences between the curvature of the retina and that of the image plane, or to minor misalignment in the camera optics. Eye movements would compound these effects, particularly if pupil dilation were insufficient. However, at this point, we are unable to separate the sources of error, most likely because they may all occur simultaneously and their effects are probably correlated with each other.

Repeatability and Sample Size

Monitoring lipofuscin levels in eyes could be performed in many situations (e.g., aging, drug, and gene therapy) with large sampling areas (such as the four-segments), since lipofuscin would be equally affected in all areas. Using the four segments has the additional benefit of balancing out some asymmetric variability, providing better repeatability. As examples, we used repeatability to estimate sample sizes for two hypothetical studies. These use our repeatability, but it is best to have estimates for the conditions of the planned study (e.g., multicenter). Example 1: does an oral drug *stop* foveal lipofuscin accumulation in healthy eyes? If we presume that the initial qAF four-segment average is 200 qAF units, which for the untreated group will increase by 5 qAF units during the 1-year study (Fig. 10), and that repeatability is 8% (thus, SD = 0.08 × 200/1.96 = 8 qAF units), for α = 0.05 and β = 0.20, the required sample size would be 41 per group. Example 2: can a drug lower the AF of patients with Stargardt's disease (average,

500 qAF units) by 75 qAF units, one fourth of the difference between them and normal qAF at age 20 y (200 qAF units)? Presuming that repeatability is 16% (twice the value used above for the normally sighted subjects in our study), the SD will be $0.16 \times 500/1.96 = 41$ qAF units, so for $\alpha = 0.05$ and $\beta = 0.20$, the required sample size would be five.

Pre-RPE Light Absorption

Quantitative fundus AF is not an absolute measurement of lipofuscin because of light losses in the ocular media and in the layers of the neurosensory retina. The measured AF would, however, correlate with the amount of lipofuscin, since the latter is the principal source of AF and the effect of all pre-RPE absorbers, outside of the fovea, is relatively small in comparison. Although some of these losses can be accounted for by appropriate protocol or corrections, some cannot.

To date, we have not corrected our data for the absorption of the ocular media. This correction is important for studies where the study population contains individuals with a large range of ages (e.g., aging and longitudinal studies). Several psychophysical[41–44] and physical[45–49] methods are available for the individual estimation of the optical density of the media. In some studies, such as a comparison of groups of young and old subjects, it may be sufficient to employ an algorithm that predicts the average media optical density for a given age.[39,50] We have used one such algorithm[39] to illustrate the effect of this correction (Fig. 10).

Absorption by photopigment reduces the excitation light to the RPE by amounts that vary with the type and quantity of photopigment, the wavelength used, and the fraction of bleached pigment. For rods, the time course of bleaching recorded in three subjects (Fig. 5) corresponded well with theoretical predictions based on the two-compartment model (with regeneration).[34–37] Cones, on the other hand, cannot be efficiently bleached with the retinal irradiances available in the two cSLOs, in part because macular pigment reduces the irradiance on the cones and because 488 nm is spectrally remote from the peak absorption by cones (550 nm). Thus, studies of foveal lipofuscin should be made with an imaging system that uses an excitation wavelength longer than 540 nm, where macular pigment absorption is very low.[21,23,51]

Furthermore, interpretation of qAF levels may have to account for light losses in the nerve fiber layer,[52] the neural layers of the retina (e.g., OCT reveals multiple reflections and hence light losses from within the retina), retinal capillaries,[53] and RPE melanin. The latter reduces the lipofuscin AF by amounts that are dependent on age, the spatial distribution of melanin, and the apical/basal distribution within the RPE cell.[54–56]We estimated that lipofuscin AF may be attenuated by a mean factor of $\approx$1.2 (age range, 20–70 y).[55,57] Unknown at this point is the contribution of melanolipofuscin[58] to the total qAF.

Conclusions

Quantitative AF imaging appears feasible with current equipment, but several technical changes could be implemented to reduce measurement errors. In addition to the new alignment software, the detection pupil could be reduced from 6 to 5 mm to decrease obstruction by the iris, automatic software rejection of degraded frames could be implemented, and additional optics could be introduced to improve the centering of the camera on the eye. Furthermore, the use of a green laser to excite the AF could minimize the effect of macular pigment and the errors associated with ocular media correction. We are developing a reflectometry method[47–49] to individually estimate the light losses in the media. Further studies will focus on more specifically identifying the sources of measurement error, optimizing image acquisition and analysis protocols, and establishing a normative database of subjects with normal retinal status. Finally, hardware installations and software development for quantitative analysis will be enhanced for portability and ease of use in multicenter studies.

By offering a clinically accessible standard against which to measure AF intensity, qAF will not only facilitate clinical research, but will also offer potential diagnostic, prognostic, and therapeutic applications.

Acknowledgments

The authors thank Tilman Otto (Heidelberg Engineering) for his numerous insights and for developing the modified alignment software.

References

1. Delori FC, Dorey CK, Staurenghi G, Arend O, Goger DG, Weiter JJ. In vivo fluorescence of the ocular fundus exhibits retinal pigment epithelium lipofuscin characteristics. *Invest Ophthalmol Vis Sci.* 1995;36:718–729.
2. Sparrow JR. Lipofuscin of the retinal pigmented epithelium. In: Holz F, Schmitz-Valckenberg S, Spaide RF, Bird A, eds. *Atlas of Fundus Autofluorescence Imaging.* Berlin, Heidelberg, New York: Springer; 2007:4–16.
3. Eagle RC, Lucier AC, Bernadino VB, Janoff M. Retinal pigment epithelial abnormalities in fundus flavimaculatus: a light and electron microscopic study. *Ophthalmology.* 1980;87:1189–1200.
4. Weng J, Mata NL, Azarian SM, Tzekov RT, Birch DG, Travis GH. Insights into the function of rim protein in photoreceptors and etiology of Stargardt's disease from the phenotype in abcr knockout mice. *Cell.* 1999;98:13–23.
5. Sun H, Nathans J. ABCR, the ATP-binding cassette transporter responsible for Stargardt macular dystrophy, is an efficient target of all-trans-retinal-mediated photooxidative damage in vitro: implications for retinal disease. *J Biol Chem.* 2001;276:11766–11774.
6. Boulton M, Rozanowska M, Rozanowski B. Retinal photodamage. *J Photochem Photobiol B.* 2001;64:144–161.
7. Ben-Shabat S, Parish CA, Vollmer HR, et al. Biosynthetic studies of A2E, a major fluorophore of retinal pigment epithelial lipofuscin. *J Biol Chem.* 2002;277:7183–7190.
8. De S, Sakmar TP. Interaction of A2E with model membranes. implications to the pathogenesis of age-related macular degeneration. *J Gen Physiol.* 2002;120:147–157.
9. Sparrow JR, Cai B, Jang YP, Zhou J, Nakanishi K. A2E, a fluorophore of RPE lipofuscin, can destabilize membrane. *Adv Exp Med and Biol.* 2006;572:63–68.
10. Schutt F, Davies S, Kopitz J, Holz FG, Boulton ME. Photodamage to human RPE cells by A2-E, a retinoid component of lipofuscin. *Invest Ophthalmol Vis Sci.* 2000;41:2303–2308.
11. Sparrow JR, Nakanishi K, Parish CA. The lipofuscin fluorophore A2E mediates blue light-induced damage to retinal pigmented epithelial cells. *Invest Ophthalmol Vis Sci.* 2000;41:1981–1989.
12. Zhou J, Kim SR, Westlund BS, Sparrow JR. Complement activation by bisretinod constituents of RPE lipofuscin. *Invest Ophthalmol Vis Sci.* 2009;50:1392–1399.
13. Sparrow JR, Boulton M. RPE lipofuscin and its role in retinal pathobiology. *Exp Eye Res.* 2005;80:595–606.
14. Delori FC. Spectrophotometer for noninvasive measurement of intrinsic fluorescence and reflectance of the ocular fundus. *Appl Opt.* 1994;33:7439–7452.
15. Delori FC, Goger DG, Dorey CK. Age-related accumulation and spatial distribution of lipofuscin in RPE of normal subjects. *Invest Ophthalmol Vis Sci.* 2001;42:1855–1866.
16. Arend OA, Weiter JJ, Goger DG, Delori FC. In-vivo fundus-fluoreszenz-messungen bei patienten mit alterabhangiger makulardegeneration. *Ophthalmologie.* 1995;92:647–653.
17. Delori FC, Staurenghi G, Arend O, Dorey CK, Goger DG, Weiter JJ. In-vivo measurement of lipofuscin in Stargardt's disease/fundus flavimaculatus. *Invest Ophthalmol Vis Sci.* 1995;36:2331–2337.
18. von Rückmann A, Fitzke FW, Bird AC. Distribution of fundus autofluorescence with a scanning laser ophthalmoscope. *Br J Ophthalmol.* 1995;119:543–562.

19. Solbach U, Keilhauer C, Knabben H, Wolf S. Imaging of retinal autofluorescence in patients with age-related macular degeneration. *Retina.* 1997;17:385–389.
20. Holz FG, Bellman C, Staudt S, Schutt F, Volcker HE. Fundus autofluorescence and development of geographic atrophy in age-related macular degeneration. *Invest Ophthalmol Vis Sci.* 2001;42: 1051–1056.
21. Morgan JIW, Hunter JJ, Masella B, et al. Light-induced retinal changes observed with high-resolution autofluorescence imaging of the retinal pigment epithelium. *Invest Ophthalmol Vis Sci.* 2008;49:3715–3729.
22. Delori FC, Fleckner MR, Goger DG, Weiter JJ, Dorey CK. Autofluorescence distribution associated with drusen in age-related macular degeneration. *Invest Ophthalmol Vis Sci.* 2000;41:496–504.
23. Spaide RF. Fundus autofluorescence and age-related macular degeneration. *Ophthalmology.* 2003;110:392–399.
24. Lois N, Halfyard AS, Bunce C, Bird AC, Fitzke FW. Reproducibility of fundus autofluorescence measurements obtained using a confocal scanning laser ophthalmoscope. *Br J Ophthalmol.* 1999;83: 276–279.
25. Lois N, Halfyard AS, Bird AC, Fitzke FW. Quantitative evaluation of fundus autofluorescence imaged "in vivo" in eyes with retinal disease. *Br J Ophthalmol.* 2000;84:741–745.
26. Cideciyan AV, Aleman TS, Swider M, et al. Mutations in ABCA4 result in accumulation of lipofuscin before slowing of the retinoid cycle: a reappraisal of the human disease sequence. *Hum Mol Genet.* 2004;13:525–534.
27. Cideciyan AV, Swider M, Aleman TS, et al. Reduced-illuminance autofluorescence imaging in ABCA4-associated retinal degenerations. *J Opt Soc Am A Opt Image Sci Vis.* 2007;24(5):1457–1467.
28. Bellmann C, Rubin GS, Kabanarou SA, Bird AC, Fitzke FW. Fundus autofluorescence imaging compared with different confocal scanning laser ophthalmoscopes. *Br J Ophthalmol.* 2003;87:1381–1386.
29. Hopkins J, Walsh A, Chakravarthy U. Fundus autofluorescence in age-related macular degeneration: an epiphenomenon? *Invest Ophthalmol Vis Sci.* 2006;47:2269–2271.
30. Schmitz-Valckenberg S, Holz F, Fitzke F. Perspectives in imaging technologies. In: Holz F, Schmitz-Valckenberg S, Spaide RF, Bird A, eds. *Atlas of Fundus Autofluorescence Imaging.* Berlin, Heidelberg, New York: Springer; 2007:332–338.
31. ANSI. American National Standard for Safe Use of Lasers (ANSI 136.1). Orlando, FL: The Laser Institute of America; 2007.
32. Delori FC, Webb RH, Sliney DH. Maximum permissible exposures for ocular safety (ANSI 2000), with emphasis on ophthalmic devices. *J Opt Soc Am A Opt Image Sci Vis.* 2007;24:1250–1265.
33. Bennett AG, Rabbetts RB. *Clinical Visual Optics.* London: Butterworths; 1984.
34. Rushton WA, Henri GH. Bleaching and regeneration of cone pigments in man. *Vision Res.* 1968;8:617–631.
35. Rushton WHA. Visual pigments in man. In: Dartnall HJA, ed. *Handbook of Sensory Physiology.* Berlin-Heidelberg-New York: Springer-Verlag;1972:364–394.
36. Liem AT, Keunen JEE, van Norren D, van der Kraats J. Rod densitometry in the aging human eye. *Invest Ophthalmol Vis Sci.* 1991;32:31–37.
37. Mainster MA. Retinol transport and regeneration of human cone photopigment. *Nat New Biol.* 1972;238:223–224.
38. Bland JM, Altman DG. Statistical method for assessing agreement between two methods of clinical measurement. *Lancet.* 1986;i: 307–310.
39. van de Kraats J, van Norren D. Optical density of the aging human ocular media in the visible and the UV. *J Opt Soc Am A Opt Image Sci Vis.* 2007;24:1842–1857.
40. Schmitz-Valckenberg S, Luong V, Fitzke F, Holz F. How to obtain the optimal fundus autofluorescence image with the confocal scanning laser ophthalmoscope. In: Holz F, Schmitz-Valckenberg S, Spaide RF, Bird A, eds. *Atlas of fundus Autofluorescence Imaging.* Berlin, Heidelberg, New York: Springer; 2007:37–47.
41. Werner JS. Development of scoptopic sensitivity and the absorption spectrum of the human ocular media. *J Opt Soc Am.* 1982; 72:247–258.
42. Sample PA, Esterson FD, Weinreb RN, Boynton RM. The aging lens: in vivo assessment of light absorption in 84 human eyes. *Invest Ophthalmol Vis Sci.* 1988;29:1306–1311.
43. Moreland JD, Torczynski E, Tripath R. Rayliegh and Moreland matches in the aging eye. *Doc Ophthalmol Proc Ser.* 1991;54:347–352.
44. Stomonyakov V, Krumov A, Vassilev A, Yankova T. An apparatus for measuring the optical density of human ocular media to blue light. *Acta Physiol Pharmacol Bulg.* 1998;23:101–105.
45. Johnson CA, Howard DL, Marshall D, Shu H. A noninvasive video-based method for measuring lens transmission properties of the human eye. *Optom Vis Sci.* 1993;70:944–955.
46. Savage GL, Johnson CA, Howard DL. A comparison of noninvasive objective and subjective measurements of the optical density of human ocular media. *Optom Vis Sci.* 2001;78:386–395.
47. Xu J, Pokorny J, Smith VC. Optical density of the human lens. *J Opt Soc Am A.* 1997;14:953–960.
48. Delori FC, Burns SA. Fundus reflectance and the measurement of crystalline lens density. *J Opt Soc Am A.* 1996;13:215–226.
49. van de Kraats J, van Norren D. Directional and non-directional spectral reflection from the human fovea. *J Biomed Opt.* 208;13: 024010.
50. Pokorny J, Smith VC, Lutze M. Aging of the human lens. *Appl Opt.* 1987;26:1437–1440.
51. Delori FC, Goger DG, Keilhauer CN, Salvetti P, Staurenghi G. Bimodal spatial distribution of macular pigment: evidence of a gender relationship. *J Opt Soc Am A Opt Image Sci Vis.* 2006;23: 521–538.
52. Knighton RW, Qian C. An optical model of the human retinal nerve fiber layer: implications of directional reflectance for variability of clinical measurements. *J Glaucoma.* 2000;9:56–62.
53. Snodderly DM, Weinhaus RS, Choi JC. Neural-vascular relationships in central retina of macaque monkeys (Macaca fascicularis). *J Neuroscience.* 1992;12:1169–1193.
54. Feeney-Burns L, Hilderbrand ES, Eldridge S. Aging human RPE: Morphometric analysis of macular, equatorial, and peripheral cells. *Invest Ophthalmol Vis Sci.* 1984;25:195–200.
55. Weiter JJ, Delori FC, Wing G, Fitch KA. Retinal pigment epithelial lipofuscin and melanin and choroidal melanin in human eyes. *Invest Ophthalmol Vis Sci.* 1986;27:145–152.
56. Boulton M, Docchio F, Dayhaw-Barker P, Ramponi R, Cubeddu R. Age-related changes in the morphology, absorption and fluorescence of melanosomes and lipofuscin granules of the retinal pigment epithelium. *Vision Res.* 1990;30:1291–1303.
57. Delori FC, Goger DG, Hammond BR, Snodderly DM, Burns SA. Macular pigment density measured by autofluorescence spectrometry: comparison with reflectometry and heterochromatic flicker photometry. *J Opt Soc America A Opt Image Sci Vis.* 2001;18:1212–1230.
58. Feeney-Burns L, Berman ER, Rothman H. Lipofuscin of human retinal pigment epithelium. *Am J Ophthalmol.* 1980;90:783–791.